Self-Assembly and Patterns in Binary Mixtures of SI Block Copolymer and PPO†

Takeji Hashimoto,* Kohtaro Kimishima, and Hirokazu Hasegawa

Department of Polymer Chemistry, Kyoto University, Kyoto 606, Japan

Received March 4, 1991; Revised Manuscript Received May 20, 1991

ABSTRACT: Self-assembled patterns were investigated for solvent-cast films of the binary mixtures of poly(2,6-dimethylphenylene oxide) (PPO) and poly(styrene-*b*-isoprene) diblock copolymers (SI) using transmission electron microscopy. The pattern formation was found to generally depend on both the *microphase transition* for the block copolymer and the liquid–liquid phase transition for the mixtures of the two polymers PPO and SI (the *macrophase transition*). The patterns with uniformly distributed microdomains in space were obtained when the microphase transition occurred prior to the macrophase transition. In this case, PPO and polystyrene (PS) block chains in SI are mixed with each other and segregated from the domains composed of polyisoprene (PI) block chains. On the other hand, when the macrophase transition occurred prior to the microphase transition, periodic concentration fluctuations of SI and PPO with a characteristic spacing of Λ_{macro} on the order of micrometers first developed probably due to spinodal decomposition. This pattern formation and growth were followed by the microphase transition, generating the microdomains of a characteristic spacing Λ_{micro} on the order of 100 nm. The pattern growth was eventually pinned down by vitrification to result in formation of a nonequilibrium structure with spatially varying microdomain morphology, a superlattice with the two spacings, Λ_{macro} and Λ_{micro}. An interesting relation between the pattern and the thermal behavior as observed by DSC was also found.

I. Introduction

Dynamics and pattern formation in ordering processes in complex fluids or condensed matters have been attracting much research interest in the field of chemical physics or physical chemistry as a problem related to nonlinear and nonequilibrium phenomena.[1,2] Along this line, blends of two kinds of homopolymers, A and B, have been studied quite extensively.[3-7] Even for such simple blends (denoted hereafter as A/B), the self-assembling patterns become extremely rich when the liquid–liquid phase separation of A/B is coupled with other kinds of phase transitions:[7] liquid–solid phase transition (i.e., crystallization[8,9]), phase transition between isotropic liquid and anisotropic liquid,[10-12] gel–sol transition,[13] and so on when at least one component, e.g., A, is crystallizable, capable of forming liquid crystals and gels, respectively.

In the case when at least one component is the block copolymer, it forms the microdomains due to the microphase separation (denoted hereafter *microphase transition*). This microphase transition in the block copolymers can be coupled with the liquid–liquid phase separation between the two constituent polymers (denoted hereafter *macrophase transition* in contrast to the microphase transition), which will again give rise to a rich variety in the self-assembled pattern, as proposed in our earlier paper.[14,15] In this paper we aim to report some results obtained along this line for mixtures of A–B diblock copolymers and C homopolymers (denoted hereafter A–B/C).

As for binary mixtures of a block copolymer and a homopolymer, most of the work has been focussed for A–B/A (or B) systems and directed toward research on miscibility and phase diagram[16-18] as well as on the effects of A on concentration fluctuations in the single-phase state,[15,19-23] on the microphase transition,[15,16,21-23] and on the size, morphology, and long-range order of the ordered microdomains[15,17,18,23-29] as well as on micelle formations.[30-39] The latter research on the effects of homopolymers on the ordered microdomains was done mostly in the regime in which only the microphase transition takes place in the self-assembling process.

The self-assembling processes and patterns in the regime in which there occurs a coupling of the microphase and macrophase transition have remained essentially unexplored up to now, even for the A–B/A systems. For the A–B/C systems, there are no systematic studies at all even on miscibility and phase diagram. The effects of the homopolymer C on the items as discussed above for the A–B/A systems also remain unexplored. The self-assembling processes and patterns are totally unexplored. In this series of work, we aim to pursue a systematic study along this line on the A–B/C systems. In this paper we report the first result of this series on binary mixtures of poly(styrene-*b*-isoprene) (SI) and poly(2,6-dimethylphenylene oxide) (PPO).

Blends of polystyrene (PS) and PPO were reported to form a single phase over the entire composition range, based on the experimental results that they exhibited single glass transitions intermediate between those of the two pure components.[40] The total miscibility between PS and PPO was tested and proven by dynamic-mechanical,[41] thermal,[41,42] and diffusion[43] measurements. Mixtures of PPO and PS-based block copolymers were investigated extensively by Tucker et al.[44-46] They found no macrophase separation between PPO and the block copolymers, PPO being completely dissolved in PS microdomains and hence uniform microdomain structures being formed. It is most crucial for us to understand their interesting observations in terms of the self-assembling processes, which generally involve the coupling of two kinds of the phase transitions. It is conceivable that their observations result from their particular sample preparation method and that their method essentially involves the microphase transition only. This point may be qualitatively clarified in our paper.

II. Possible States of Mixtures

It may be worthy to visualize the possible states of mixtures, before going into detailed discussion. Figure 1

* Author to whom correspondence should be addressed.

† Presented in part before the 37th Annual Meeting of the Society of Polymer Science, Nagoya, Japan, May 1988. Hasegawa, H.; Hashimoto, T. *Polym. Prepr. (Jpn. Soc. Polym. Sci., Jpn.)* **1988**, *37*, 1107.

0024-9297/91/2224-5704$02.50/0

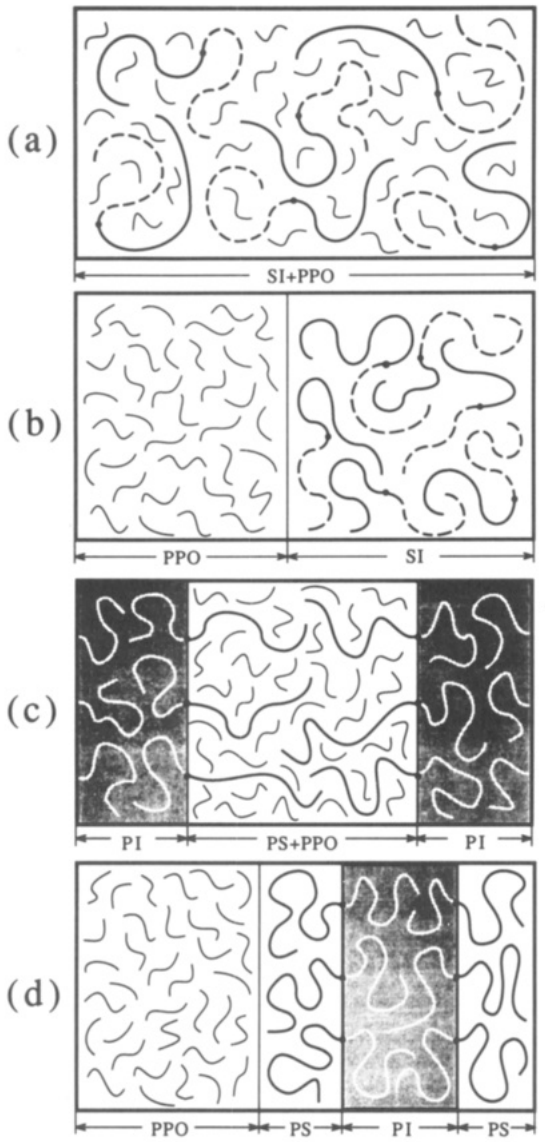

Figure 1. Schematic representation of the possible states of SI/PPO mixtures. (a) Single-phase state. SI and PPO are mixed at the molecular level. (b) Phase-separated state. SI is in the disordered state and phase-separated from PPO. (c) SI is microphase-separated, and PPO is preferentially solubilized in the PS domains. (d) Phase-separated into SI-rich and PPO-rich macrophases. SI is microphase-separated into PS-rich and PI-rich microdomains.

sketches the possible equilibrium states. Part a sketches the single-phase state in which SI is in the disordered (the single-phase) state and mixed with PPO at the molecular level. Part b sketches the phase-separated state in which SI is in the disordered state and phase-separated from PPO, generating the SI-rich phase and the PPO-rich phase. This state is formed in the case when only the macrophase transition is involved by either the nucleation growth process[47] or the spinodal decomposition (SD) process.[48] There are many intermediate states evolved during the ordering process, leading to state b.

Part c sketches the state in which SI undergoes the microphase transition to form the domains rich in polystyrene (PS) block chains and those rich in polyisoprene (PI) block chains and PPO is preferentially solubilized in the PS domains. The preferential solubilization is due to the fact that PPO is totally miscible with PS[40-42] but not with PI. This state is formed in the case when only the microphase transition occurs, and the microphase transition generates a number of possible microdomain morphologies with a

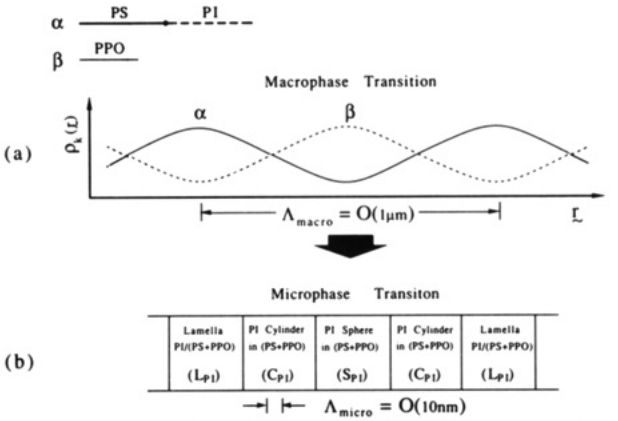

Figure 2. (a) Profiles of the periodic concentration fluctuations of polymer α or SI (solid curve) and polymer β or PPO (dotted curve) with a spacing of Λ_{macro} (on the order of 1 μm) developed by the SD process in the macrophase transition. (b) Modulated pattern or a pattern with the superlattice of the spatially varying microdomains with a short periodicity of Λ_{micro} (on the order of 10 nm) superimposed over the periodic concentration fluctuation corresponding to a.

long-range spatial order, e.g., spherical, cylindrical, and lamellar microdomains,[49] as well as their intermediate structures such as the tetrapod network[50] or OBDD,[51] lamellar catenoid,[52] mesh,[53] and strut (3d network).[53]

Part d sketches the phase-separated state in which both the microphase and macrophase transition occur. SI forms the PS-rich and PI-rich microdomains as a consequence of the microphase transition. This SI phase coexists with the PPO macrophase as a consequence of the macrophase transition. The SI phase is the phase rich in SI in which a minor fraction of PPO may be preferentially solubilized in PS-rich microdomains, and the PPO-phase is the phase rich in PPO in which a minor fraction of SI is solubilized either in the disordered state as in the part a or in the ordered state to form a microdomain different from that in the SI-rich phase. Again there are a number of possible microdomain morphologies with the long-range spatial order in the SI-rich phase as in the case of the state sketched in part c. As in the case of part b, a number of possible intermediate states will be formed in this self-assembling process via the micro- and macrophase transitions, investigation of which is a primary theme in this paper.

Although not included in Figure 1, there may be states a′, b′, and d′, corresponding to the states a, b, and d, respectively, in which the SI dissolved in PPO forms micelles or vesicles.[32-39]

Let us take a step further on the discussion given above and consider here a possible intermediate structure formed in the self-assembling process of SI/PPO. What kind of patterns will be formed if the self-assembling process involves first the macrophase transition via SD and subsequently the microphase transition? The SD process may develop periodic concentration fluctuations of SI (or polymer α) and PPO (or polymer β) with a spacing of Λ_{macro} on the order of 1 μm as sketched in Figure 2a, depending on time spent for SD at a given phase-separation condition. If this macrophase transition is followed by the microphase transition and if PPO and PS are mixed at the molecular level to form the microdomains of PS and PPO mixed with each other and segregated from the microdomains of PI, the self-assembling process may generate a modulated pattern or a pattern with superlattice as shown in Figure 2b in which the microdomain morphology with a short periodicity of Λ_{micro} on the order of 10 nm spatially varies with the long spacing of Λ_{macro}. If the regions richest in SI form the lamella of PS and

Table I
Characteristics of Specimens Used in This Work

Poly(2,6-dimethylphenylene oxide)

code	M_n[a]	M_w/M_n[a]
PPO	1.17×10^4	3.64

Poly(styrene-*b*-isoprene) Diblock Copolymers

code	M_n[b]	M_w/M_n[a]	PS/PI (w/w)[c]	$M_{n,PS}$[d]	morphology[e]
HY-12	5.24×10^5	1.16	52/48	2.7×10^5	lamella
B-2	1.76×10^5	1.26	85/15	1.5×10^5	PI sphere

[a] Measured by size-exclusion chromatography, and M_n is equivalent to standard polystyrene. [b] Measured by membrane osmometry. [c] Measured by elemental analysis. [d] Calculated from M_n and the composition PS/PI (w/w). [e] Determined from transmission electron microscopy and small-angle X-ray scattering analysis.

PPO and that of PI, which are alternating (denoted hereafter as L_{PI} morphology), and those poorest in SI form the spherical domains of PI dispersed in the matrix of PS and PPO (denoted hereafter as S_{PI} morphology), the regions in between form the cylindrical domains of PI in the matrix of PS and PPO (denoted hereafter as C_{PI} morphology). Such a process may generate a pattern comprised of spatially varying microdomain morphology of L_{PI}, C_{PI}, S_{PI}, C_{PI}, and L_{PI} with the spacing of Λ_{micro} in the long spacing of Λ_{macro}. The length scale Λ_{macro} and details of the pattern at the large scale such as the sharpness of the morphological transition and relative volume fraction of the region having each microdomain morphology may depend on the phase-separation conditions such as time and temperature. The long-range order of the microdomains at the length scale of Λ_{micro} may depend also on the phase-separation conditions.

III. Experimental Methods

Characteristics of specimens used in this study were summarized in Table I. The number-average molecular weight, M_n, was measured by size-exclusion chromatography for PPO as an equivalent value with standard polystyrene samples and by membrane osmometry for SI block copolymers. The heterogeneity index, M_w/M_n, was measured by size-exclusion chromatography. Two kinds of SI block copolymers, coded as HY-12 and B-2 used in this work, have, respectively, morphologies of the alternating lamellar microdomain (Figure 6) and spherical microdomains of PI dispersed in the PS matrix (Figure 3a) when they are solvent-cast using toluene. Note that the molecular weight of PPO is much smaller than the molecular weights of PS block chains for both HY-12 and B-2. Thus, in the case when HY-12 and B-2 form the microdomains, PPO may tend to be uniformly solubilized in the PS microdomains, according to the solubilization criterion found by Inoue et al.[26,54] Since the content of PS is 85 wt % for B-2 and 52 wt % for HY-12 and PPO is miscible with PS, B-2 is expected to be more miscible with PPO than HY-12.

The film specimens of the blends of HY-12/PPO with compositions 100/0, 80/20, 60/40, 30/70, and 10/90 w/w and of B-2/PPO with compositions 100/0, 90/10, 70/30, 50/50, 30/70, and 10/90 w/w were prepared by casting from toluene solutions containing the total amount of the polymers by ca. 5 wt %. The toluene solutions were homogeneous and prepared by dissolving the polymers at ca. 50 °C.

The patterns formed in the solvent-cast films were examined by transmission electron microscopy (TEM) with the ultrathin sections. The as-cast films of the mixtures were stained with osmium tetraoxide (OsO_4) vapor, embedded in epoxy resin, and ultramicrotomed by using an LKB 4800A ultrotome with a glass knife at room temperature. The ultrathin sections of ca. 50 nm thickness were picked up on copper grids with carbon-coated formvar supporting film, stained again with OsO_4 vapor, and subjected to observation under a Hitachi H-600S transmission electron microscope at an accelerating voltage of 100 kV.

Differential scanning calorimetry (DSC) was performed with a DSC 3200 by Mac Science (Japan) at a heating rate of 20 °C/m. A test piece used for the DSC experiment was cut from the same cast films of the mixtures of PPO and the block copolymers as those used for the electron microscopy. For the DSC measurements on the mixtures of PPO and PS homopolymer ($M_n = 2.04 \times 10^5$, $M_w/M_n = 1.05$), the test specimens were prepared by dissolving the polymer mixtures in toluene, precipitating the mixture with a large quantity of methanol, and carefully drying the precipitates in a vacuum oven. The glass transition temperatures reported below refer the onsets of the glass transitions.

IV. Results and Discussion

The patterns formed in the solvent-cast films may be classified into those controlled by the self-assembling process via the microphase transition, e.g., B2/PPO, as will be discussed in section IV-A, and those controlled by that involving the coupling between the macro- and microphase transition, e.g., HY-12/PPO, as will be discussed in section IV-B. These two kinds of patterns will be contrasted in this section.

A. Self-Assembled Patterns Controlled by Microphase Transition. In order to generate the patterns controlled by the microphase transition only, we selected the B2/PPO systems and prepared the films by a rapid solvent evaporation. The thin-film specimens were prepared by pouring the 5 wt % toluene solution on a cover glass and by evaporating the solvent within ca. 1 min with aid of an air blower. The thin films thus prepared were transparent. Since PPO is totally miscible with PS but is immiscible with PI and PI is a minority component in SI, the macrophase transition is expected to be suppressed. Hence, the microphase transition may occur prior to (or at a lower concentration than) the macrophase transition during the solvent evaporation process. The rapid solvent evaporation was aimed at bringing the homogeneous solution into the higher concentration regime where the macrophase transition occurs under the condition in which the preceding microphase transition affects as little as possible.

Figure 3 shows typically the experimental results for the B2/PPO films as observed by the TEM method. As shown in part a, the neat B2 film has the S_{PI} morphology in which PI spheres are selectively stained dark by OsO_4 in the matrix of the unstained PS block chains. When PPO is mixed with an increasing fraction, (i) the S_{PI} morphology is maintained, but (ii) the volume fraction of the PI spheres decreases, as clearly observed in the series of micrographs. Moreover, (iii) the spatial organization of the PI spheres remains regular and uniform over the significantly wide area observed by TEM. These three pieces of evidence imply that PPO is uniformly mixed with PS block chains, forming the matrix of the S_{PI} morphology as a consequence of the microphase transition, but that there are no hints indicating the effect of the macrophase transition on the patterns. In other words, the regions rich in SI or PPO were never observed in the micrographs. Thus the rapid solvent evaporation method used in our experiments turned out not to be sufficiently rapid to avoid the effect of the microphase transition on the pattern formation.

The uniform solubilization of PPO in the PS matrix and the absence of the macrophase transition was able to be further confirmed by the DSC experiments done for the same film specimens as in Figure 3. As seen in Figure 4, there is only a single glass transition temperature (T_g) between the glass transition temperature of the PS homopolymer ($T_{g,PS}$ = 103 °C) and that of the PPO homopolymer ($T_{g,PPO}$ = 254 °C). Moreover, this T_g sys-

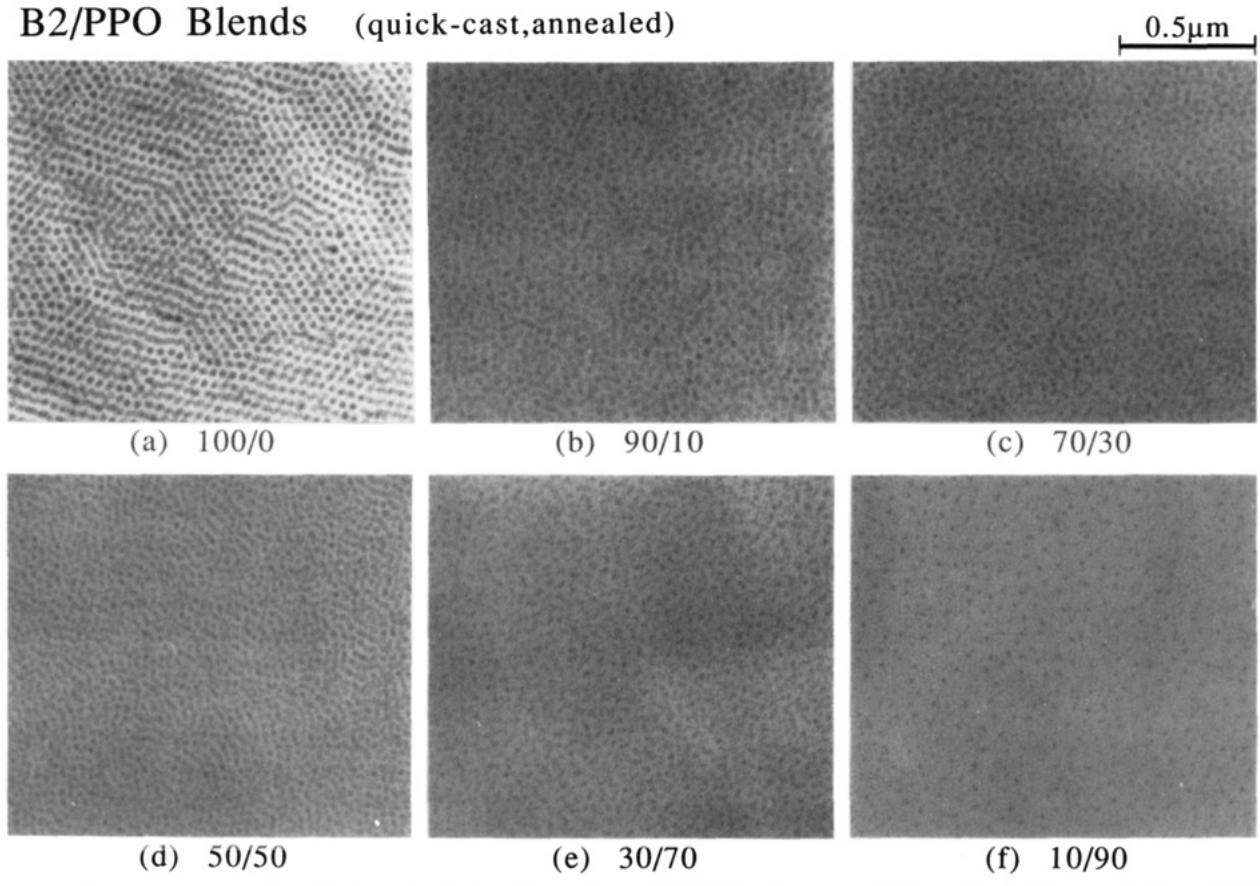

Figure 3. Electron micrographs of OsO_4-stained ultrathin sections of B2/PPO mixtures quickly cast from toluene solutions: (a) 100/0, (b) 90/10, (c) 70/30, (d) 50/50, (e) 30/70, (f) 10/90 (wt %/wt %).

tematically shifts with an increasing fraction of PPO. This shift was compared with that for the mixtures of the PS homopolymer and PPO (PS/PPO). Figure 5 shows the comparison of the two sets of T_g's as a function of the PPO fraction in which the data for B2/PPO and PS/PPO are shown by the filled and open circles, respectively. The two sets of data are identical within experimental accuracy, implying that the PS block chains in SI are uniformly mixed with PPO as the PS homopolymer does. Thus, the patterns shown in Figure 3, which were generated by the particular thermal history, are controlled primarily by the self-assembling process via the microphase transition only.

B. Self-Assembled Patterns Controlled by a Coupling of the Macro- and Microphase Transition. In order to find the effects of the macrophase transition on the patterns, we selected the mixtures of HY-12/PPO and prepared the solvent-cast films using the 5 wt % toluene solutions by slowly evaporating the solvent. In this slow solvent evaporation, the films of ca. 0.5 mm thickness were prepared in a Petri dish by evaporating the solvent at a natural rate in a covered glass vessel at a controlled temperature of 30 °C for about 1 week. It is expected that the increased fraction of the PI block chain in SI promotes the macrophase transition and that the slow solvent evaporation promotes the effects of the macrophase transition on the pattern formation by expanding the time spent in the two-phase regime prior to the vitrification set-in during the solvent evaporation. The films thus prepared were turbid.

The neat SI specimen (HY-12) exhibits the alternating lamellar microdomain morphology as shown in Figure 6. The patterns formed in the solvent-cast films of the HY-12/PPO mixtures are shown in Figure 7 as a function of the blend compositions: (a) 80/20, (b) 60/40, (c) 30/70,

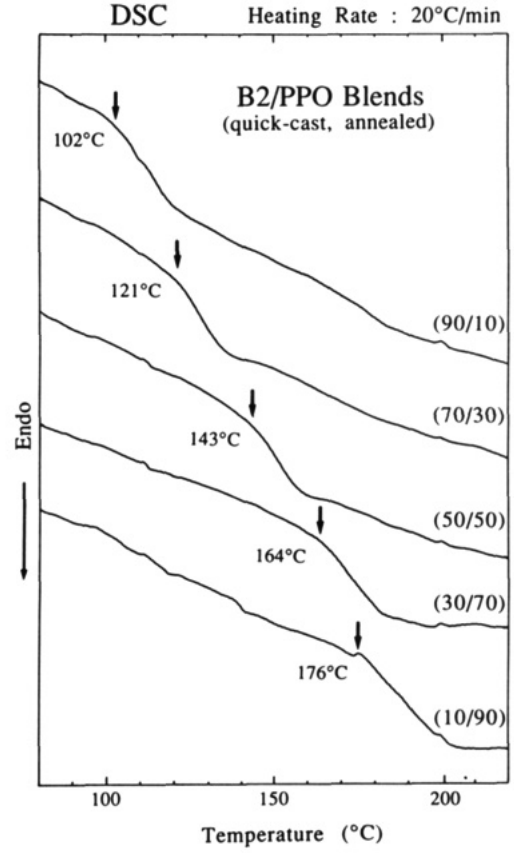

Figure 4. DSC thermograms for the films of B2/PPO 90/10, 70/30, 50/50, 30/70, and 10/90 (wt %/wt %) mixtures quickly cast from toluene solutions. T_g (onset) of each mixture is shown by an arrow.

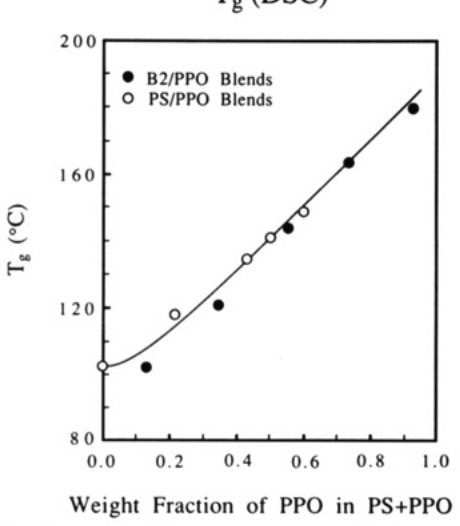

Figure 5. Glass transition temperatures obtained from DSC measurements (onset temperature) as a function of the weight fraction of PPO in the PPO + PS phase for B2/PPO (filled circles) and PS/PPO (open circles) blends.

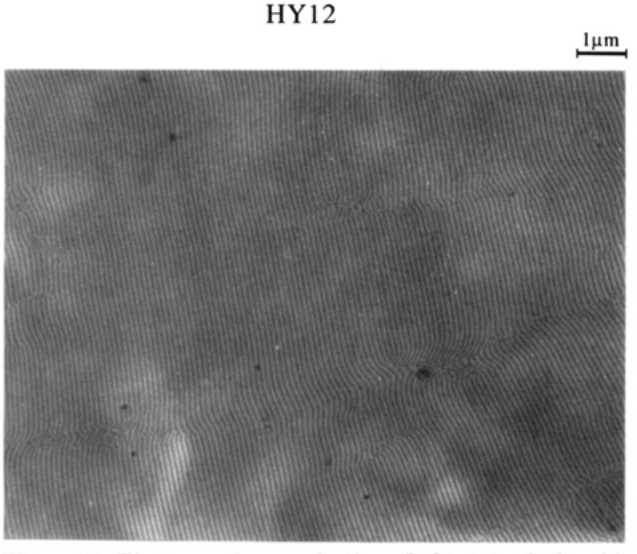

Figure 6. Electron micrograph of an OsO_4-stained ultrathin section of HY12 slowly cast from toluene solution.

and (d) 10/90. Regardless of the blend composition, these patterns have the following overall characteristics: (i) they are composed of the microdomains, but (ii) they are heterogeneous such that the local microdomain morphology is spatially varying as in parts a–c or the local microdomain morphology is identical everywhere (spheres) but the spatial arrangement of them is locally varying as in part d. The pattern in part a comprises L_{PI}, C_{PI}, and S_{PI}, while that in part b comprises C_{PI} and S_{PI}. In all cases PPO are mixed with PS block chains, forming the bright domains. The pattern c comprises percolating networks of SI-rich domains in the matrix of the PPO-rich domains. The PPO-rich domains from the S_{PI} morphology. The microdomain morphology in the SI-rich domains is not well-understood at present and cannot be clearly classified into a well-known microdomain morphology such as spheres and cylinders. The pattern in part d comprises the PI spheres in the matrix of PPO and PS, but there are regions rich in the PI spheres (and hence rich in the SI block copolymer) and those rich in PPO (or poor in the PI spheres) that appeared bright. The heterogeneous patterns a–d commonly imply that the self-assembling process is affected by the macrophase transition and that this macrophase transition is coupled by the microphase transition.

Pattern c comprised of the percolated network of SI-rich domains might be interpreted as the one formed by segregation of SI as a result of solvent-induced spherulitic crystallization of PPO during the solvent evaporation process; viz., the noncrystallizable SI may be segregated into the boundaries between neighboring PPO spherulites. If this is the case, the network pattern is expected to be observed also for the pattern shown in part d for the HY-12/PPO mixture with the 10/90 composition, since this mixture should be more easily crystallizable than the 30/70 mixture. However, in reality the percolating network cannot be observed for the 10/90 mixture, which may imply that the percolating network is formed more likely through the macrophase transition than through the liquid–solid transition (i.e., the crystallization).

Figure 8 shows the TEM micrograph for the 80/20 mixture, showing a much wider area than that in Figure 7a. The micrograph shows the pattern in which the microdomain morphology changes spatially, with the long period Λ_{macro} on the order of micrometers, from the L_{PI} morphology (as in the regions marked A) to the C_{PI} morphology (as in the regions marked B or C) and to the S_{PI} morphology (as in the regions marked D). The microdomains have the spacing of $\Lambda_{micro} \cong 100$ nm. The microdomain morphology appearing in region B may locally have "mesh structure" (M_{PI}).[53] The M_{PI} structure is similar to the alternating lamella of PI block chains and that of PS block chains plus PPO homopolymers, but there are catenoid channels comprised of PS and PPO that traverse through the PI lamellae and that interconnect the adjacent lamellae comprised of PS and PPO. Thus the two-dimensional PI meshes are dispersed in the matrix of PS and PPO. The appearance of the dark dots aligned in linear array in region B resembles the M_{PI} structure observed for another system.[53] The lamella catenoid structure[52] in which there are catenoid channels traversing through both types of the lamellae (e.g., the PI channels traversing through the lamellae of PS and PPO and the channels of PS and PPO traversing through the PI lamellae) appears to be less probable in this case. Here we suggest the mesh structure as a possible structure but will leave detailed investigation on it as a future work. Region C appears to be closer to the C_{PI} morphology than M_{PI}.

Figure 9 shows the pattern for the HY-12/PPO mixture with the 80/20 composition over an even wider area. The spatially varying morphology with the superlattice structure is evident. In the micrograph there are regions marked D′, which contain less PI spheres than region D, though a number of small dark spheres might be lost during the entire image reconstruction process leading to the final photoprinting.

The micrographs shown in Figures 7a, 8, and 9 clearly indicate that the PPO volume fraction spatially varies more or less periodically with the characteristic spacing of Λ_{macro} on the order of micrometers. The lamellar morphology should exist in the regions poorest in PPO and the S_{PI} morphology in the regions richest in PPO. The boundary over which such morphological change occurs is sufficiently wide and on the order of a few hundred nanometers. These observations lead us to conclude that the patterns are formed first by the macrophase transition via the SD mechanism, which is followed by the microphase transition and eventually by vitrification, in the self-assembling process involved by the solvent evaporation.

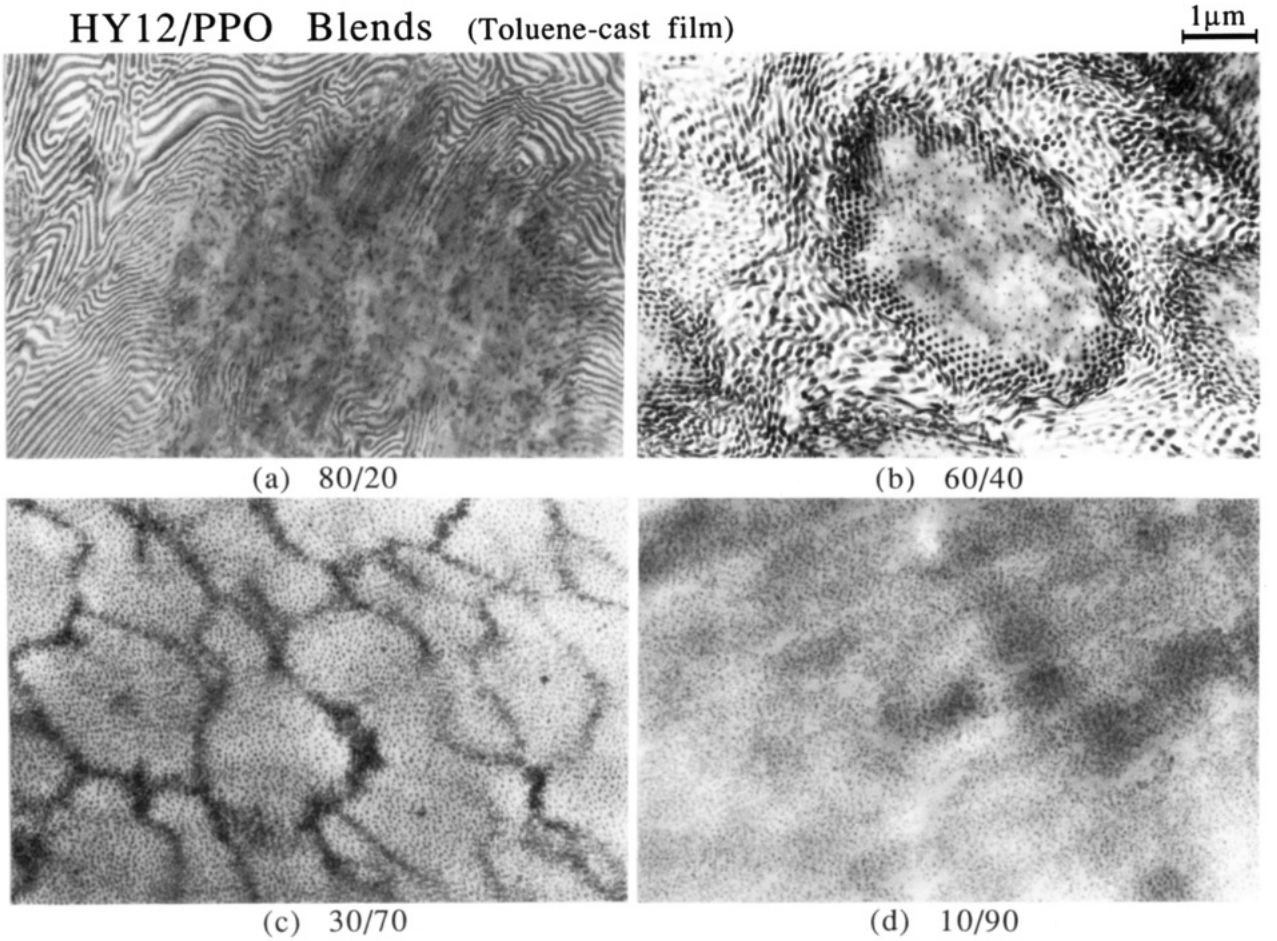

Figure 7. Electron micrographs of OsO_4-stained ultrathin sections of HY12/PPO mixtures slowly cast from toluene solutions: (a) 80/20, (b) 60/40, (c) 30/70, (d) 10/90 (wt %/wt %).

Figure 10 shows a TEM micrograph for the mixture of HY-12/PPO 60/40, showing the self-assembled pattern over an area wider than that shown in Figure 7b. The micrograph again shows the spatially varying microdomain morphology with Λ_{macro} on the order of micrometers and $\Lambda_{micro} \cong 100$ nm. Compared with the mixture of HY-12/PPO 80/20 in Figures 7a, 8, and 9, this mixture has a larger overall volume fraction of PPO, and hence its SI-rich regions after the macrophase transition may have a smaller volume fraction of the PI block chains relative to that of the PS block chains plus PPO than the mixture of HY-12/PPO 80/20. Thus, it forms the C_{PI} morphology in the SI-rich regions after the microphase transition. Similarly in the PPO-rich domains, the S_{PI} morphology is developed. Again the boundaries between the domains of different morphologies appear to extend over a distance much larger than R_g, radii of gyration of the constituent polymers. It should be noted that the free surface of the specimen marked by arrows and running from the top-right to the left-bottom corner of the micrograph is always actually covered by a monomolecular layer of polyisoprene, appearing as a dark thin layer, although a portion of the free surface appears uncovered by the PI layer in the micrograph. This is consistent with our earlier experimental finding for the neat SI block copolymer having the C_{PI} morphology in bulk and best interpreted as a consequence of PI having the lowest surface tension.[55]

The spatial concentration fluctuations of PPO as sketched in Figure 2 turns out to be the origin of the unique self-assembled patterns as shown in Figure 7. The fluctuations would also cause unique thermal behavior because they give rise to the spatial variation of the glass transition temperature, T_g, of the phase comprising PS and PPO. Figure 11 shows the DSC thermograms in the temperature range between 70 and 220 °C for the HY-12/PPO (80/20) mixture (solid line), whose pattern is shown in Figures 7a, 8, and 9, and for the B-2/PPO (70/30) mixture (broken line) prepared by the same method as in Figure 3, as a reference. Note that these two mixtures have the almost identical average-volume ratio of PS and PPO, the ratio PS/PPO being 67/33 and 66/34 for HY-12/PPO (80/20) and B-2/PPO (70/30), respectively. The thermogram for the latter mixture shows a single T_g (≅120 °C), corresponding to T_g of the matrix phase of PPO and PS in which they are uniformly mixed as discussed in section IV-A. However, the thermogram for the former mixture shows no discontinuous change, indicating the spatial variation of T_g corresponding to PS and PPO, consistent with the TEM observations.

C. Interpretation on Self-Assembling Process. Our interpretation on the self-assembling patterns discussed in sections IV-A and -B is summarized below on the basis of the schematic phase diagrams as shown in Figure 12 in which parts a and b are concerned with the mixtures of B2/PPO and HY-12/PPO, respectively. The solid and broken lines schematically represent the phase boundaries for the microphase and macrophase transition, respectively.

Since B2 is rich in the PS block chain, which is miscible with PPO, the macrophase transition is expected to be suppressed relative to the microphase transition. When the solvent evaporates from a dilute solution of a given blend composition specified at point D during the film preparation process, the state of the solution changes along the line ABCD. The microphase transition may occur at point B prior to the macrophase transition at point C and

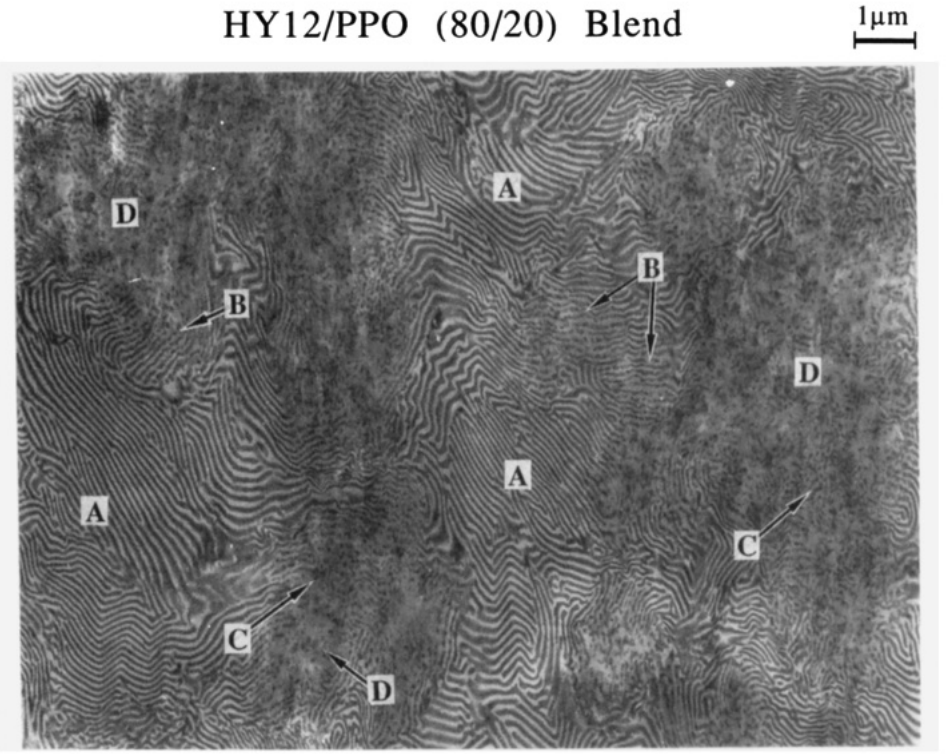

Figure 8. Electron micrograph of an OsO_4-stained ultrathin section of an HY12/PPO 80/20 (wt %/wt %) mixture slowly cast from toluene solution.

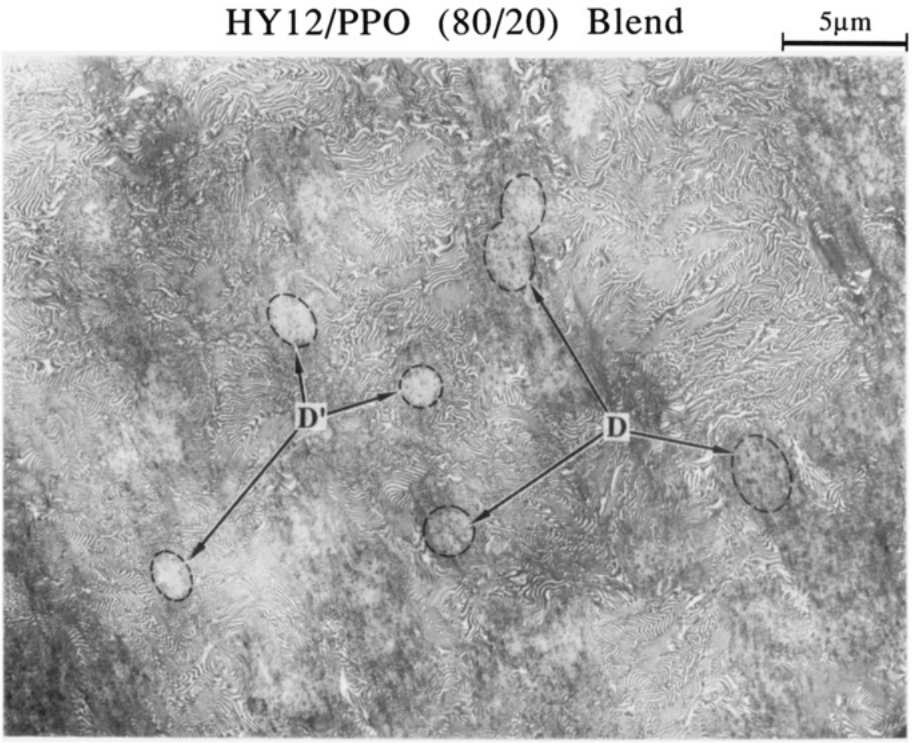

Figure 9. Same as Figure 8 but with a lower magnification.

generates the microdomain morphology of S_{PI} swollen with toluene. B2/PPO forms S_{PI} regardless of the PPO content, because the net weight fraction of the PI block forming the spheres is in the range of 0.015–0.12.

Once the S_{PI} microdomains are formed, the broken line for the macrophase transition loses its significance. It has a physical significance only when the solution in a state on line AB is quenched suddenly in a state on line CD and when the latter state on line CD is still above the glass transition temperature. Under this situation, both the macrophase and microphase transition can occur in principle and affect the self-assembly. Our rapid solvent-cast method, however, does not obviously bring the solution in this regime. The solvent-evaporation rate is still sufficiently slow so that the self-assembly is expected to be controlled by the microphase transition.

Once the S_{PI} morphology is formed, it hardly grows, owing to the severe nonequilibrium effect inherent to this morphology, as discussed in detail elsewhere.[56,57] Thus, the PI spheres formed near point B rather shrink in terms of their size and intersphere distances upon further evaporation of the solvent along the line BD to result in

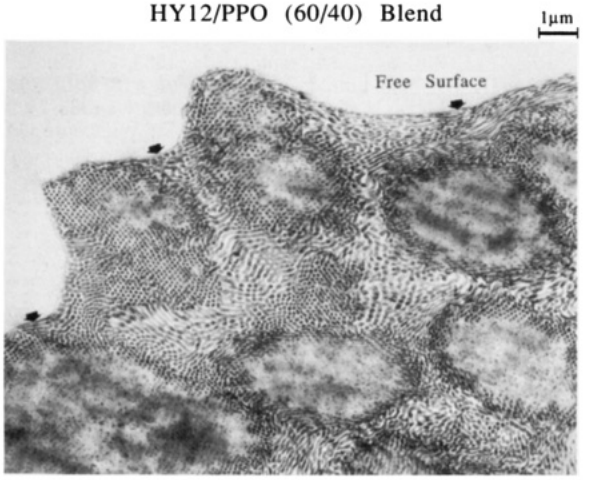

Figure 10. Electron micrograph of an OsO_4-stained ultrathin section of an HY12/PPO 60/40 (wt %/wt %) mixture slowly cast from toluene solution.

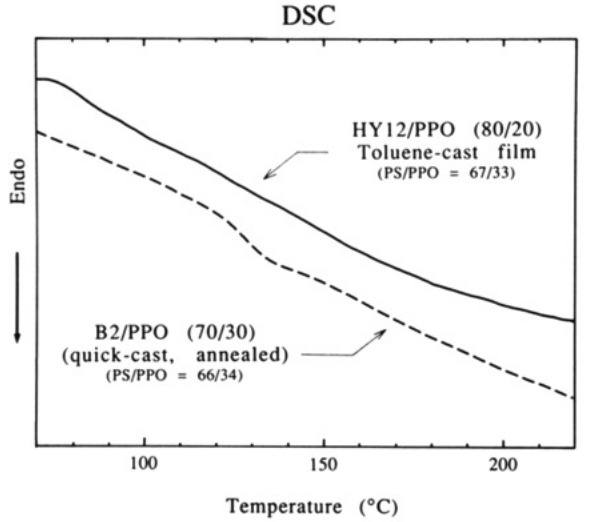

Figure 11. DSC thermograms of the toluene-cast films of an HY12/PPO (80/20) mixture (solid curve) and a B2/PPO (70/30) mixture (broken curve). The PS/PPO ratio is 67/33 for the former and 66/34 for the latter.

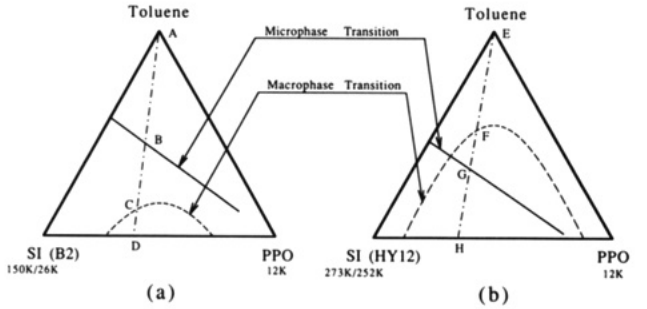

Figure 12. Schematic phase diagrams for (a) B2/PPO/toluene and (b) HY12/PPO/toluene ternary mixtures at a given temperature (e.g., the temperature of film casting). The solid lines and broken curves indicate hypothetical critical concentrations for the microphase and macrophase transitions, respectively. The dash-and-dot lines indicate the path for the film-casting process.

the pattern as found in Figure 3. The size of the PI spheres and the intersphere distance are essentially pinned down at the instance when the S_{PI} morphology is formed in the solution.[56,57] Thus, the decrease in the size of the PI spheres with an increasing PPO fraction as shown in Figure 3 reflects the phenomenon when the PI spheres are formed in the solution.[54] The decrease of the PI spheres with an increasing fraction of PPO is due to the swelling of the PS

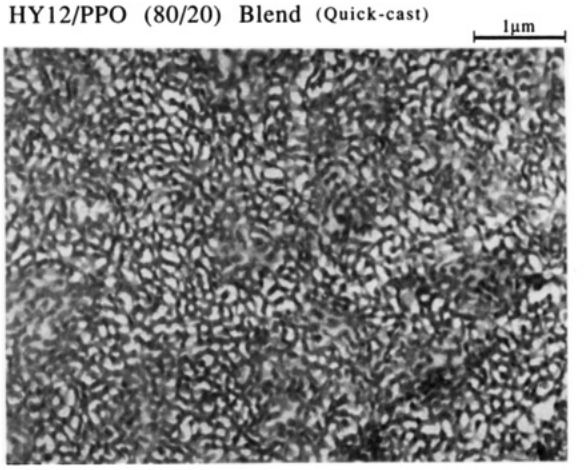

Figure 13. Electron micrograph of an OsO_4-stained ultrathin section of an HY12/PPO 80/20 (wt %/wt %) mixture quickly cast from toluene solution.

block chains by PPO.[26,27] The swelling increases the curvature of the interface between PI solution and the solution of PS and PPO, as discussed in detail elsewhere.[26]

A greater fraction of PI block in HY-12, which is immiscible with PPO, as compared with B2, is expected to promote the macrophase transition relative to the microphase transition, as shown schematically in Figure 12b. When the blend with a composition specified at point H is cast into films from a dilute solution, the state of the solution changes along the line EFGH. The solution may undergo the macrophase transition via SD in the process of passing the line FG, prior to the microphase separation, generating the spatial concentration fluctuations of SI and PPO with the spacing Λ_{macro}. During the solvent-evaporation process, the fluctuations will grow further in terms of its amplitude and Λ_{macro}. The concentration eventually reaches that in which the microphase separation starts to occur, and microdomains are formed in the process corresponding to the line GH. The variation of the local concentration of the PI block against that of PS plus PPO, which was generated by the macrophase transition, would cause the variation of the microdomain morphology in space after the microphase transition. The pattern growth is eventually pinned by vitrification to result in the self-assembled pattern in the solid film as summarized in Figure 7.

As the volume fraction of PPO increases, the volume fraction of the PI block in the regions rich in SI decreases, and the local morphology may change from L_{PI} (Figure 7a for 80/20), C_{PI} (Figure 7b for 60/40), and S_{PI} morphology (Figure 7d for 10/90). The corresponding local morphology for the 30/70 mixture in the percolating SI-rich domain appears to be a morphology that cannot be well-defined, intermediate between C_{PI} and S_{PI}. The local morphology of PPO-rich regions is S_{PI} for the 80/20, 60/40, and 30/70 mixtures and featureless PPO domains for the 10/90 mixture.

Since the time evolution of the concentration fluctuations with the large spacing Λ_{macro} is a slow process, there may be a chance that the solution can be supersaturated, without a significant effect of the macrophase transition in the process corresponding to the line FG, into a state on the line GH where the microphase transition is triggered and the microdomain is formed, if the solvent evaporation rate is sufficiently rapid. Figure 13 shows a TEM micrograph for the mixture of HY-12/PPO (80/20) prepared by the rapid solvent-cast method as used to prepare the B2/PPO specimens. The micrograph shows

a uniform microdomain structure as characterized by "strut" morphology,[53] i.e., the 3d network of the PI microdomain (St_{PI}) in the matrix of PPO and PS. There are no regions obviously rich in PPO or SI, indicating little effect of the macrophase transition on the pattern. The St_{PI} morphology may be reasonable in view of the weight fraction of the PI block (0.38), which may be higher than that for the C_{PI} morphology but lower than that for the L_{PI} morphology.

V. Concluding Remarks

Self-assembled patterns are reported for the solvent-cast film of the binary mixtures of PPO and SI, using toluene as a solvent and a low molecular weight PPO compared with the molecular weight of the PS block. The self-assembling processes leading to such unique patterns as discussed in sections IV-A and -B were qualitatively discussed in terms of the microphase and macrophase transition occurring in the systems during the solvent-evaporation process. Especially the transition that occurs first is pointed out to be important for the final pattern observed in the solid films. Further research on the following points deserves future studies: effects of the molecular weights of PPO and SI and of solvent on the pattern, the real-time analysis of the ordering process, investigation of Flory's χ-parameters among the constituent polymers and solvent, and phase diagrams for the macrophase and microphase transition.

Acknowledgment. This work is supported in part by a Grant-in-Aid for Scientific Research in Priority Areas "New Functionality Materials, Design, Preparation and Control" (02205066) from the Ministry of Education, Science and Culture, Japan.

References and Notes

(1) Komura, S., Furukawa, H., Eds. *Dynamics of Ordering Processes in Condensed Matter*; Plenum Press: New York, 1988.
(2) Onuki, A., Kawasaki, K., Eds. *Dynamics and Patterns in Complex Fluids*; Springer-Verlag: Berlin, 1990.
(3) Nose, T. *Phase Transitions* **1987**, *8*, 245.
(4) Hashimoto, T. *Phase Transitions* **1988**, *12*, 47.
(5) Takenaka, M.; Tanaka, K.; Hashimoto, T. In *Contemporary Topics in Polymer Science, Vol. 6, on Multiphase Macromolecular Systems Symposium*; Culbertson, W. M., Ed.; Plenum Press: New York, 1989; p 363.
(6) Utracki, L. A. *Polymer Alloys and Blends*; Hanser: Munich, 1990.
(7) Hashimoto, T. In *Materials Science and Technology, Vol. 12, Structure and Properties of Polymers*; VCH: Weinheim, Germany, Chapter 6, in press.
(8) Inaba, N.; Sato, K.; Suzuki, S.; Hashimoto, T. *Macromolecules* **1986**, *19*, 1690.
(9) Inaba, N.; Yamada, T.; Suzuki, S.; Hashimoto, T. *Macromolecules* **1988**, *21*, 407.
(10) Nakai, A.; Shiwaku, T.; Hasegawa, H.; Hashimoto, T. *Macromolecules* **1986**, *19*, 3008.
(11) Hasegawa, H.; Shiwaku, T.; Nakai, A.; Hashimoto, T. Reference 1, p 457.
(12) Kyu, T.; Zhuang, P. *Polym. Commun.* **1988**, *29*, 99.
(13) Kawanishi, K.; Komatsu, M.; Inoue, T. *Polymer* **1987**, *28*, 981.
(14) Tanaka, H.; Hashimoto, T. *Polym. Commun.* **1988**, *29*, 212.
(15) Hashimoto, T.; Tanaka, H.; Hasegawa, H. In *Molecular Conformation and Dynamics of Macromolecules in Condensed Systems*; Nagasawa, M., Ed.; Elsevier: Amsterdam, The Netherlands, 1988; p 257.
(16) Roe, R.-J.; Zin, W. C. *Macromolecules* **1984**, *17*, 189.
(17) Hong, K. M.; Noolandi, J. *Macromolecules* **1983**, *16*, 1083.
(18) Whitmore, M. D.; Noolandi, J. *Macromolecules* **1985**, *18*, 2486.
(19) Tanaka, H.; Sakurai, S.; Hashimoto, T.; Whitmore, M. D. *Polymer*, in press.
(20) Douy, A.; Mayer, R.; Rossi, J.; Gallot, B. *Mol. Cryst. Liq. Cryst.* **1969**, *7*, 103. Skoulios, A.; Helffer, P.; Gallot, Y.; Selb, J. *Makromol. Chem.* **1971**, *148*, 305.
(21) Tanaka, H.; Hashimoto, T. *Macromolecules*, in press.
(22) Nojima, S.; Roe, R.-J. *Macromolecules* **1987**, *20*, 1866.
(23) Owens, J. N.; Gancarz, I. S.; Koberstein, J. T.; Russell, T. P. *Macromolecules* **1989**, *22*, 3388.
(24) Quan, X.; Gancarz, I.; Koberstein, J. T.; Wignall, G. D. *Macromolecules* **1987**, *20*, 1431.
(25) Berney, C. V.; Cheng, P.-L.; Cohen, R. E. *Macromolecules* **1988**, *21*, 2235.
(26) Hashimoto, T.; Tanaka, H.; Hasegawa, H. *Macromolecules* **1990**, *23*, 4378.
(27) Tanaka, H.; Hasegawa, H.; Hashimoto, T. *Macromolecules* **1991**, *24*, 240.
(28) Tanaka, H.; Hashimoto, T. *Macromolecules*, in press.
(29) Winey, K. I.; Thomas, E. L. In *Material Research Society*; Schaefer, D. W., Mark, J. E., Eds.; Elsevier, New York, 1990; Vol. 171, p 255.
(30) Shull, K. R.; Kramer, E. J.; Hadziioannou, G.; Tang, W. *Macromolecules* **1990**, *23*, 4780.
(31) Thomas, E. L.; Winey, K. I. *Proc. ACS Div. Polym. Mater.: Sci. Eng.* **1990**, *62*, 686.
(32) Noolandi, J.; Hong, K. M. *Macromolecules* **1983**, *16*, 1443.
(33) Leibler, L.; Pincus, P. A. *Macromolecules* **1984**, *17*, 2922.
(34) Rigby, D.; Roe, R.-J. *Macromolecules* **1984**, *17*, 1778.
(35) Rigby, D.; Roe, R.-J. *Macromolecules* **1986**, *19*, 721.
(36) Roe, R.-J. *Macromolecules* **1986**, *19*, 728.
(37) Kinning, D. J.; Winey, K. I.; Thomas, E. L. *Macromolecules* **1988**, *21*, 3502.
(38) Witten, T. A.; Milner, S. T.; Wang, Z. G. Reference 5.
(39) Berney, C. V.; Cheng, P. L.; Cohen, R. E. *Macromolecules* **1988**, *21*, 2235.
(40) Cizek, E. P. (assigned to General Electric Co.) U.S. Patent 3,383,435, May 14, 1968.
(41) Stoelting, J.; Karasz, F. E.; MacKnight, W. J. *Polym. Eng. Sci.* **1970**, *10*, 133.
(42) Bair, H. E. *Polym. Eng. Sci.* **1970**, *10*, 247.
(43) Composto, R. J.; Kramer, E. J.; While, D. M. *Macromolecules* **1988**, *21*, 2580.
(44) Kambour, R. P. (assigned to General Electric Co.) U.S. Patent 3,639,508, Feb 1, 1972.
(45) Shultz, A. R.; Beach, B. M. *J. Appl. Polym. Sci.* **1977**, *21*, 2305.
(46) Tucker, P. S.; Barlow, J. W.; Paul, D. R. *Macromolecules* **1988**, *21*, 1678, 2794, 2801.
(47) Cahn, J. W.; Hilliard, J. E. *J. Chem. Phys.* **1959**, *31*, 688.
(48) Cahn, J. W.; Hilliard, J. E. *J. Chem. Phys.* **1958**, *29*, 258.
(49) Molau, G. E. In *Block Polymers*; Aggarwal, S. L., Ed.; Plenum Press: New York, 1970; p 79.
(50) Hasegawa, H.; Tanaka, H.; Yamasaki, K.; Hashimoto, T. *Macromolecules* **1987**, *20*, 1651.
(51) Thomas, E. L.; Alward, D. B.; Kinning, D. J.; Martin, D. C.; Handlin, D. L., Jr.; Fetters, L. J. *Macromolecules* **1986**, *19*, 2197.
(52) Thomas, E. L.; Alward, D. B.; Henkee, C. S.; Hoffman, D. *Nature* **1988**, *334*, 598.
(53) Hashimoto, T.; Koizumi, S.; Hasegawa, H.; Izumitani, T.; Hyde, S. T., submitted to *Macromolecules*.
(54) Inoue, T.; Soen, T.; Hashimoto, T.; Kawai, H. *Macromolecules* **1970**, *3*, 87.
(55) Hasegawa, H.; Hashimoto, T. *Macromolecules* **1985**, *18*, 589; *Polymer*, in press.
(56) Shibayama, M.; Hashimoto, T.; Kawai, H. *Macromolecules* **1983**, *16*, 16.
(57) Mori, K.; Hasegawa, H.; Hashimoto, T. *Polymer* **1990**, *31*, 2368.

Registry No. PPO, 24938-67-8; (I)(S) (block copolymer), 105729-79-1; 2,6-xylenol (homopolymer), 25134-01-4.